

# THE DEVELOPMENT OF MESOSCOPIC STRUCTURAL ANALYSIS FOR MECHANICAL PROPERTY REDUCTION OF CONCRETE DAMAGED BY EXPANSION CRACKING DUE TO ASR

T. MIURA<sup>\*</sup>, Y. YAMAMOTO<sup>†</sup> AND H. NAKAMURA<sup>††</sup>

<sup>\*</sup> Nagoya University  
Nagoya, Japan  
e-mail: t.miura@civil.nagoya-u.ac.jp

<sup>†</sup> Nagoya University  
Nagoya, Japan  
e-mail: y.yamamoto@civil.nagoya-u.ac.jp

<sup>††</sup> Nagoya University  
Nagoya, Japan  
e-mail: hikaru@nagoya-u.jp

**Key words:** ASR, expansion cracking behavior, Compression property, 3D-RBSM

**Abstract:** In this study, the analytical system coupled with reaction producing model and expansion model for ASR and mesoscopic structural analysis was developed to evaluate both of expansion cracking behaviors and mechanical property change due to ASR. The proposed ASR model considered the random location of aggregates can simulate both of expansion behavior and cracking behavior. In addition, expansion cracking behavior and the reduction of compressive property were simulated for compression tests of concrete deteriorated by expansion crack due to ASR. As a result, it was confirmed that smaller cracks generate and propagate firstly, and gradually larger cracks propagate in association with increase of expansion strain in sequence. Furthermore, the reduction tendency of compressive strength due to several expansion strain can be estimated with a high degree of accuracy.

## 1 INTRODUCTION

It is well-known that Alkali-Silica-Reaction (ASR) is one of deterioration phenomena that generates expansion pressure around reactive aggregate by chemical reaction with alkali content. As this deterioration progresses, it was reported that expansion crack occurs in concrete and leads to rebar breaking. In addition, the expansion crack can accelerates the penetration of deterioration factors from external environment. Therefore, it is very important to evaluate and predict both structural performance and durability performance for concrete structure damaged by ASR.

In the present day, the expansion mechanism of ASR is not fully understood yet. The foremost hypothesis for ASR expansion was the water absorption of reaction products. Current concept of ASR expansion mechanism [1] is that reaction products react with Ca of cement paste and they will becomes high viscosity products around reactive aggregate named rim and, after that, the expansion pressure generates from reactive aggregate due to producing reaction products. At this moment, the enormous experimental investigations have been carried out to establish the expansion mechanism which comprehensively interprets signature expansion behavior due to ASR.

On the other hands, some of researcher have developed numerical method for reconstructing expansion behavior of ASR. Those numerical approaches are to reconstruct expansion behaviors itself [2] and to evaluate the structural performance by means of coupling with structural analysis [3, 4]. Recently, the numerical analysis coupled with expansion model and mesoscopic structural analysis to comprehend the expansion mechanism of ASR [5].

To comprehend the expansion mechanism, the authors believe the high possibility of mesoscopic structural analysis because it can evaluate the mechanical information such as expansion pressure and expansion crack and it is difficult to obtain them by means of experiment. Then, in this study, the numerical analysis was developed to reconstruct the expansion cracking behaviors and mechanical properties reduction due to ASR by 3D-RBSM.

## 2 MODELING OF EXPANSION BEHAVIORS DUE TO ASR

In this chapter, the modeling for producing reaction products and expansion crack propagation behavior due to ASR are indicated. Figure 1 shows proposed analytical flow. In this study, the analytical system that composed by reaction product calculation by initial information related to ASR, expansion strain calculation from reaction product amount, and

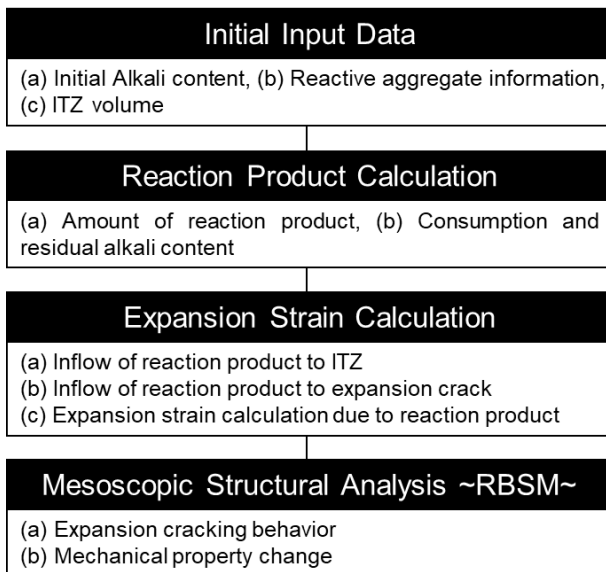


Figure 1: Analytical flow

mesoscopic structural analysis was developed.

### 2.1 Calculation for reaction product

The initial information related to ASR are initial alkali content, reactive aggregate amount, and its size distribution. Initial alkali content is calculated by eq.1 based on  $\text{Na}_2\text{O}$  amount in pore solution proposed by Diamond et.al. [6].

$$C_{in} = 0.699 \times \text{Na}_2\text{O}_{eq} + 0.017 \quad (1)$$

where,  $C_{in}$  is the initial Alkali content (mol/L),  $\text{Na}_2\text{O}_{eq}$  is Alkali amount of pore solution (%).

The reaction with alkali content and reactive aggregate is applied by Uomoto model [7] that is a reaction model which the surface area of reactive aggregate where contacts with alkali decreases with a time.

$$x = \sqrt{k_{TR}tC} \quad (2)$$

$$a_i = 1 - \left(1 - \frac{x}{R_i}\right)^3 \quad (3)$$

$$T_{pr} = A \sum B_i k_1 a_i \quad (4)$$

$$V_{gel} = \alpha T_{pr} \quad (6)$$

where,  $x$ : reaction layer of reactive aggregate from aggregate surface (mm),  $k_{TR}$ : reaction rate constant ( $5.1 \times 10^{-11}$  cm<sup>2</sup>/h),  $t$ : time (h),  $C$ :alkali content (mol/L),  $T_{pr}$ : reaction product amount contributes to expansion (mol/L),  $A$ : unit amount of reactive aggregate (g/L),  $B_i$ : the volume ratio of aggregate which diameter is  $R_i$  in whole aggregate,  $k_1$ : the conversion factor of reaction product amount from reaction volume ratio ( $=0.0166$  mol/g),  $a_i$ : reaction volume ratio of aggregate which diameter is  $R_i$ ,  $V_{gel}$ : the volume of reaction product which can contribute to expansion,  $\alpha$ : the conversion factor of volume from reaction product amount ( $=6 \times 10^5$  mm<sup>3</sup>/mol), respectively.

### 2.2 Calculation for expansion strain

Regarding to Uomoto model [7], the reactive product cannot contribute to expansion until

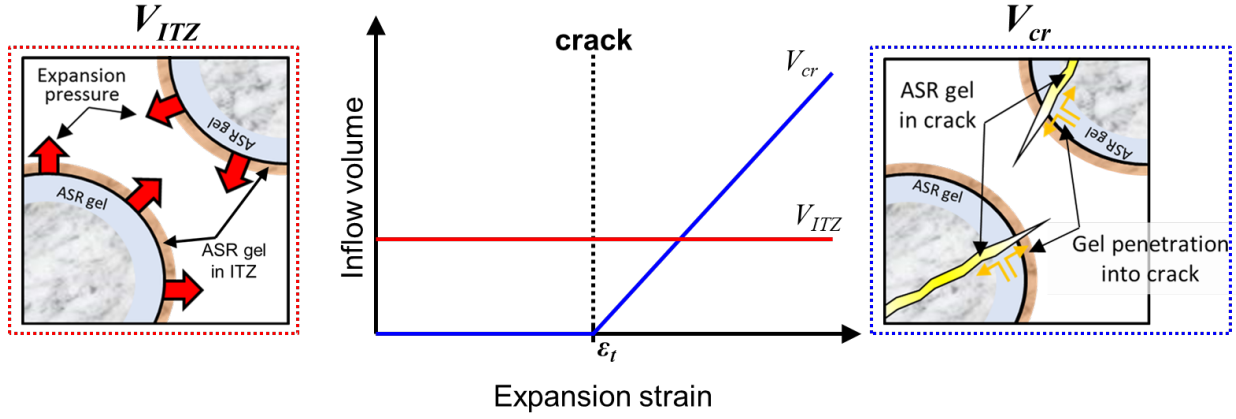


**Figure 2:** the concept of inflow effect of reactive product  $V_{ITZ}$  and  $V_{cr}$

reaction product amount  $k_{IA}$  exceeds the certain capacity. This indicates the latent periods that the expansion pressure doesn't generate due to the inflow of reaction product to aggregate interface. Thus concept has been applied to the other numerical simulation for ASR. This proposed analysis was considered that the inflow effect is attributed to both ITZ and expansion crack due to ASR in order to clearly distinguish their effect as shown in Figure 2. In particular, the inflow effect of reaction product to ITZ is calculated by the ITZ volume when the thickness of ITZ is 0.03mm as shown in eq.5. This volume is constant if expansion strain increases. After filled in the ITZ volume by reaction product, expansion strain can generate. In addition, the inflow effect of reaction product to expansion crack is calculated by the crack volume which possesses one reactive aggregate. This inflow effect changes with increase of crack width. The inflow effect by ITZ influences to expansion behaviors at initial stage of ASR deterioration and the inflow effect by expansion crack becomes larger as ASR expansion progresses. Based on this concept, the inflow effect was assumed.

$$V_{ITZ} = \left( \frac{4\pi}{3} \right) \left\{ (D_i + T_{ITZ})^3 - D_i^3 \right\} \quad (5)$$

where,  $V_{ITZ}$ : the inflow effect of reaction products to ITZ ( $\text{mm}^3$ ),  $D_i$ : diameter of reactive aggregate (mm).

Finally, by using  $V_{gel}$ ,  $V_{ITZ}$  and  $V_{cr}$ , the expansion strain can be calculated by following equation.

$$\varepsilon_{ASR} = \frac{V_{gel} - \beta V_{ITZ} - \gamma V_{cr}}{V_{elm}} \quad (7)$$

when,  $V_{cr}$ : the inflow effect of reaction product to expansion crack ( $\text{mm}^3$ ),  $V_{elm}$ : the volume of one reactive aggregate,  $\beta$ : the influence factor of  $V_{ITZ}$ ,  $\gamma$ : the influence factor of  $V_{cr}$ , respectively.

The influence factors of  $\beta$  and  $\gamma$  are equal to 1.0. This physical meaning is that reaction products can penetrate into those space and expansion strain cannot be generated until completely filling.

### 2.3 Expansion model for ASR

In the previous investigation by the authors [8], the macroscopic expansion strain can be strongly influenced by expansion model. For example, the two different type of expansion model are assumed. One case is that all elements were set to expansion strain and another one is that the certain distributed elements were set to expansion strain so as to describe the actual reactive aggregate location. Only latter case can simulate both macroscopic

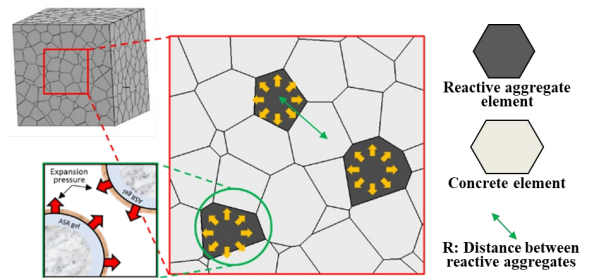


**Figure 3:** Distributed expansion model

expansion strain and expansion cracking behaviors somehow controlling the analytical parameters such as  $\alpha$ ,  $\beta$  and  $\gamma$ . Furthermore, this expansion model named distributed expansion model as shown in Figure 3 can describe the constraint effect on expansion behavior. This kind of approach have been modeled by Alnaggar et.al. [5]. In this analysis, they proposed ASR model with directly modeling the reactive aggregate particles to describe expansion rate and expansion cracking behaviors. Thus, the special location of reactive aggregate is very important to reconstruct both macroscopic expansion strain and expansion cracking behavior.

In this study, the authors attempted to evaluate not only reconstruct the expansion mechanism of ASR but also the change of structural performance of reinforced concrete structure damaged by ASR. Then, the expansion due to reactive product was modeled briefly by randomly selecting the element in consistent with the volume of reactive aggregate and applying the averaged expansion strain to each element. The specific calculation method is as below. Firstly, the volume ratio of reactive aggregate in concrete was calculated from size distribution and the ratio of reactive aggregate. Next, the distance between reactive aggregates:  $R$  was defined. In first selection,  $R$  was set to more than ten times of element size. First reactive aggregate was randomly selected in concrete and second reactive aggregate was, subsequently, selected where was distant from first one more than  $R$ . If there no selectable element in concrete, the value of  $R$  decreased gradually until the volume ratio of reactive aggregate in concrete is lower than

experimental one. Thus, the reactive aggregate location was distributed so as not to be close them each other.

#### 2.4 Mesoscopic structural analysis -RBSM-

RBSM (Rigid Body Spring Model) developed by Kawai [9] is one of the discrete element methods. Bolander and Saito [10] introduced a random geometry to the RBSM element mesh using Voronoi tessellation and have shown that the model can simulate the crack patterns, the deformation and the load capacity of concrete materials and RC structures successfully. The authors have already developed constitutive models for the three-dimensional RBSM (Yamamoto et al. [11]) as mentioned above, in order to quantitatively evaluate the mechanical responses including not only detailed cracking information but also softening and localization failures, and have shown that the model can well simulate the cracking and failure behaviors of reinforced concrete members.

In the RBSM, concrete is modeled as an assemblage of rigid particles interconnected by springs arranged along their interfaces (Figure 4). The crack pattern is strongly affected by the mesh design since the cracks initiate and propagate through the interface of particles. Therefore, a random geometry of rigid particles is generated by a Voronoi diagram (Figure 4), which reduces mesh bias on the initiation and propagation pass of potential cracks. Each rigid particle has three translational and three rotational degrees of freedom defined at the centroid of the particles (Figure 4). The interface of two particles is divided into several triangles with a center of gravity and vertices of

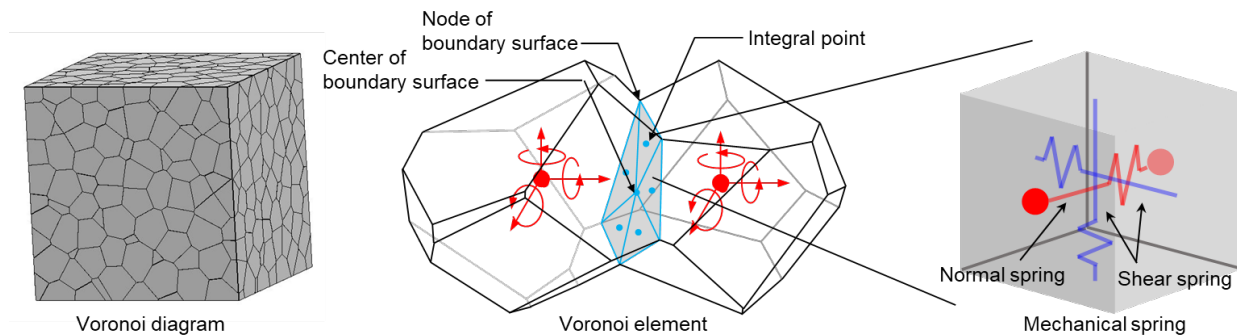


Figure 4: RBSM and Voronoi particle

the surface. One normal and two shear springs are set at the center of each triangle. By distributing the springs in this manner the model accounts for the effects of bending and torsional moment without any rotational springs (Yamamoto et al. [11]).

## 2.2 Constitutive models

The constitutive models for normal and shear spring are shown in Figure 5. The tensile model for normal springs is shown in Figure 5(a). Figure 5(b) shows the stress–strain relation for compression of normal springs that was modeled as an S-shape curve. The shear stress strain relation represents the combination of two shear springs as shown in Figures 5(c)–(e).

The material parameters as described above have been calibrated by conducting parametric analyses comparing with the test results of

uniaxial tension, uniaxial compression, hydrostatic compression and tri-axial compression. The parametric analyses include a variety of specimen size, shape, the mesh size and concrete strengths. The calibrated parameters are shown in Table 1 and Table 2. These parameters are recommended for normal strength concrete. For the simplification, the material parameters are assumed to be uniformly distributed over a discretized concrete region. From a practical application perspective, although the mesh size is preferable to be larger for the sake of reducing computational cost, it has been confirmed that the proposed model can simulate the crack propagation and the localized compression failure in post-peak region in the case of that the average mesh size is around approximately 10–30 mm (Yamamoto et al. [11]).

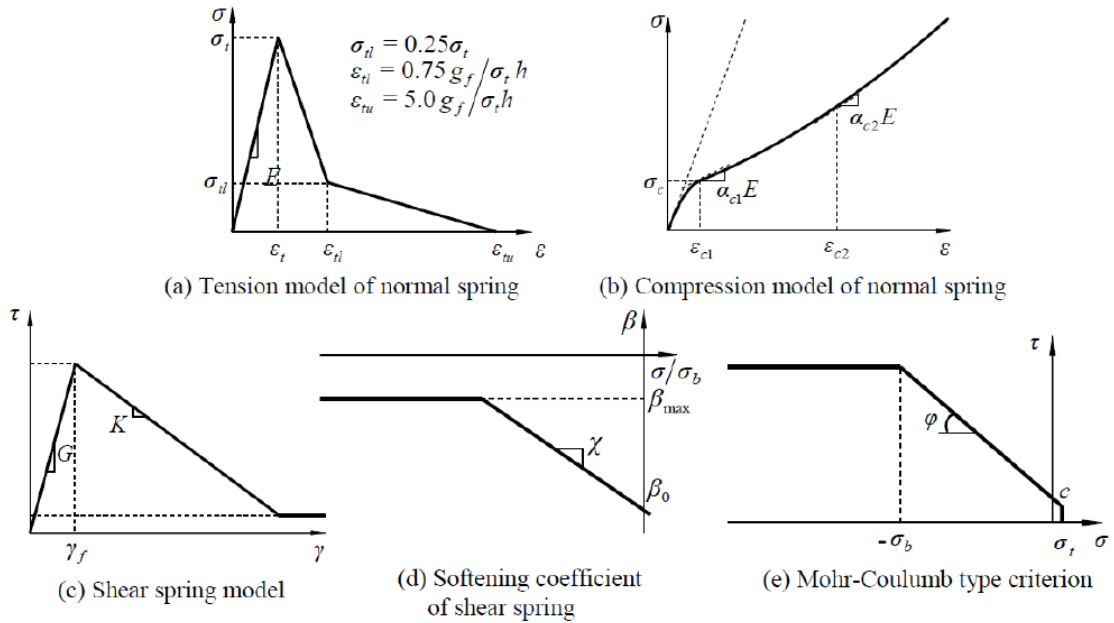


**Figure 5:** Constitutive model for concrete

**Table 1:** Constitutive law of normal mechanical spring

$E$ (N/mm <sup>2</sup> )	$\sigma_t$ (N/mm <sup>2</sup> )	$g_f$ (N/mm)	$\sigma_c$ (N/mm <sup>2</sup> )	$\varepsilon_{c2}$	$\alpha_{c1}$	$\alpha_{c2}$
$1.4E^*$	$0.8f_t^*$	$0.5G_F^*$	$1.5f_c^{**}$	-0.015	0.15	0.25

**Table 2:** Constitutive law of shear mechanical spring

$G$ (N/mm <sup>2</sup> )	$c$ (N/mm <sup>2</sup> )	$\varphi$ (degree)	$\sigma_b$ (N/mm <sup>2</sup> )	$\beta_0$	$\beta_{max}$	$\chi$	$\kappa$
$0.35E$	$0.14f_c^*$	37	$1.00f_c^{**}$	-0.05	-0.025	-0.01	-0.3

### 3 VALIDATION OF PROPOSED MESO-SCOPIC MODEL FOR ASR

#### 3.1 Objective experiment

The analytical objective is the experimental results carried out by Sakai [12]. They conducted compression tests with concrete deteriorated by ASR expansion and investigated the expansion cracking behavior quantitatively. The specimen size was  $\Phi 100 \times 200 \text{mm}$  and  $100 \times 100 \times 200 \text{mm}$ . The mix proportion of concrete is shown in Table. The reactive aggregate was set to only coarse aggregate and crushed andesite were used which aggregate was justified detrimental aggregate by JIS A 1145. The amount of  $\text{Na}_2\text{O}_{\text{eq}}$  was  $8 \text{kg/m}^3$ . The curing duration was 28 days by sealed curing and, after that, acceleration test for ASR where temperature was kept in  $40^\circ\text{C}$  and  $100\% \text{RH}$ . During the acceleration test, the expansion strain was measured at the lateral surface. When strain value became 100, 500, 1000, 1500, 2000, 3000, and  $4000 \mu$ , the compression tests were carried out with deteriorated concrete in both types of specimen. In fact, the compressive strength after  $100 \mu$  expansion was bigger than sound concrete specimen due to hydration. So, in this study, the initial compressive strength was set to that of after  $100 \mu$  expansion which is  $64.5 \text{MPa}$ . In addition, by using prism specimens after expansion, they were cut at the center part by concrete cutter and the internal crack observations were conducted after impregnating with epoxy resin containing fluorescent agent.

#### 3.2 Analytical condition

In this paper, the change in expansion strain and the change of compression property were evaluated by longitudinal shaped analytical model. The average element size is  $10 \text{mm}$ . In fact, the analytical parameters for RBSM except for compressive strength was defined by JSCE specification equations.

Firstly, the parametric analysis for calibrating the analytical parameter of ASR expansion model in a way that is consistent with the change in experimental expansion strain. By

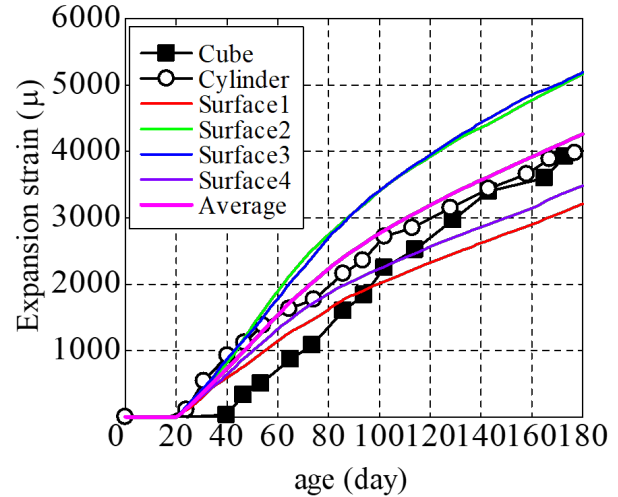


Figure 6: the change in expansion strain

the way, the decided parameters were already shown in chapter 2. The correspondence of the change in expansion strain in experiment and calculated by proposed analysis was shown in Figure 6. In fact, the analytical results of expansion strain at the four lateral surfaces which are same location of objective experiment were indicated. According to this figure, the averaged expansion strain was almost same tendency in comparison to experimental results while the variation between the results of four lateral surface seems to be big. By the way, the starting point of expansion strain can be controlled by  $\beta$  which is the influence factor of  $V_{ITZ}$ . In this paper, the value of  $\beta$  is equal to 1.0 to be simplified the analytical parameter. Thereby, it can be judged that the analytical result calculated with  $\beta$  is 1.0 which indicates starting point of expansion strain after filling reaction product to  $V_{ITZ}$  was consistent with the result of cylindrical experimental results. Thus, the proposed analysis can easily fit to experimental macroscopic expansion behavior.

Based on this analytical results, the expansion cracking behaviors and the change of compressive property will be evaluated.

#### 3.3 Validation of expansion cracking behavior due to ASR

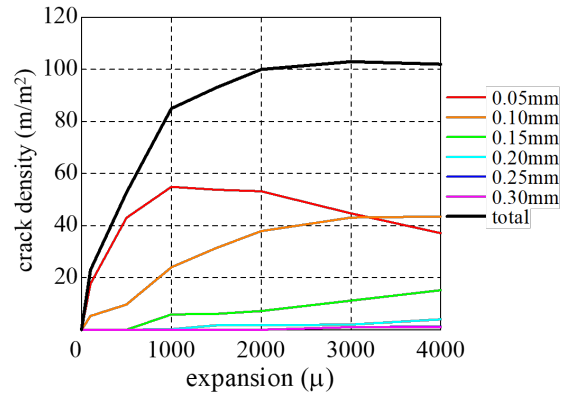
The change in expansion cracking behavior of each crack width with increase of expansion strain was shown in Figure 7. In this objective

experiment, the crack width was categorized by 0.05, 0.10, 0.15, 0.20, 0.25, 0.30mm and the total crack length of each width were accumulated at the cross-sectional area. And, the crack density of each width were calculated by that accumulated total crack length were divided by crass-sectional area. On the other hands, in the analysis, the total crack area, which is same as cracked boundary surface area of element, can be evaluated. Therefore, the crack density of each crack width were calculated by that accumulated total crack area were divided by the volume of analytical model. In fact, there are no difference between experimental and analytical crack density intrinsically. In addition, another notification is that the definition of crack width is slightly different between experiment and analysis. In this objective experiment, the representative crack width seems to have the certain range of crack width, and the range is not, however, clear. So, it was defined that the analytical ranges of crack width were less than 0.05, 0.05-0.10, 0.10-0.15, 0.15-0.20, 0.20-0.25, and more than 0.25mm.

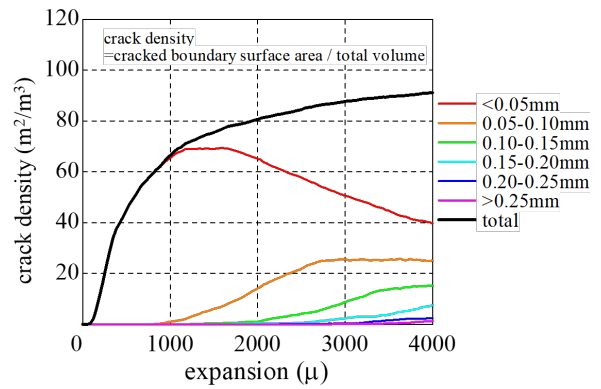
According to this figure, the crack density of less than 0.05mm crack width started to increase from about 90 $\mu$  expansion until 1100 $\mu$  expansion and it decreased with increase of expansion strain. As expansion strain became larger, the crack density of wider crack width increased in sequence. In addition, the total crack density in analytical result firstly increased and seems to become constant with increase of expansion strain gradually. This tendency is very similar to experimental results while analytical result of crack density of smaller crack width is relatively higher.

### 3.4 Validation of the reduction of compressive property due to ASR

The compressive property after 0, 500, 1000, 2000, and 4000 $\mu$  expansion were simulated by proposed analysis. The expansion cracking behavior after each expansion strain is shown in Figure 8. According these pictures, expansion crack generated gradually with increase of expansion strain and larger crack locally distributed. The change of compression



(a) experimental data [12]



(b) analytical results

**Figure 7:** the relationships between crack density of expansion crack of each crack width and expansion strain

strength and the correspondence of compression stress and lateral and vertical strain relationships in experiment and analysis were shown in Figures 9 and 10. According to these figures, it can be confirmed that the proposed analysis can reconstruct the reduction of compression strength with high accuracy. As looking at the stress strain relationships as shown in Figure 10, the change of stiffness until 1000 $\mu$  expansion was similar to experimental results. However, the initial stiffness indicated non-linearity as expansion strain increases. The possible reason is that the analysis ignores the existence of reactive products in expansion crack, and/or the time lag until compression stress transferred is longer than experiment because smaller crack width calculated by proposed analysis was relatively higher.

By using proposed analysis, the change in expansion cracking behaviors and the change of

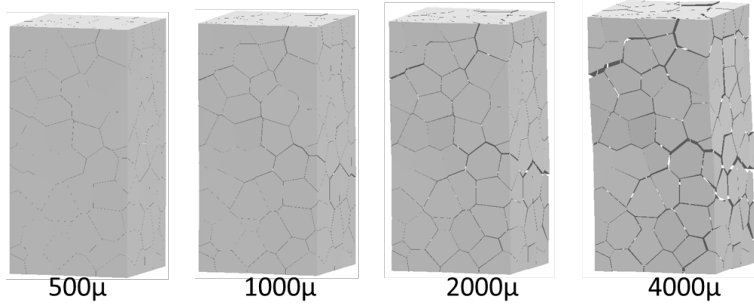


Figure 8: expansion cracking behavior

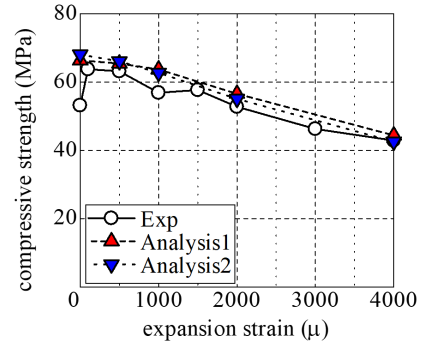


Figure 9: change of compressive strength

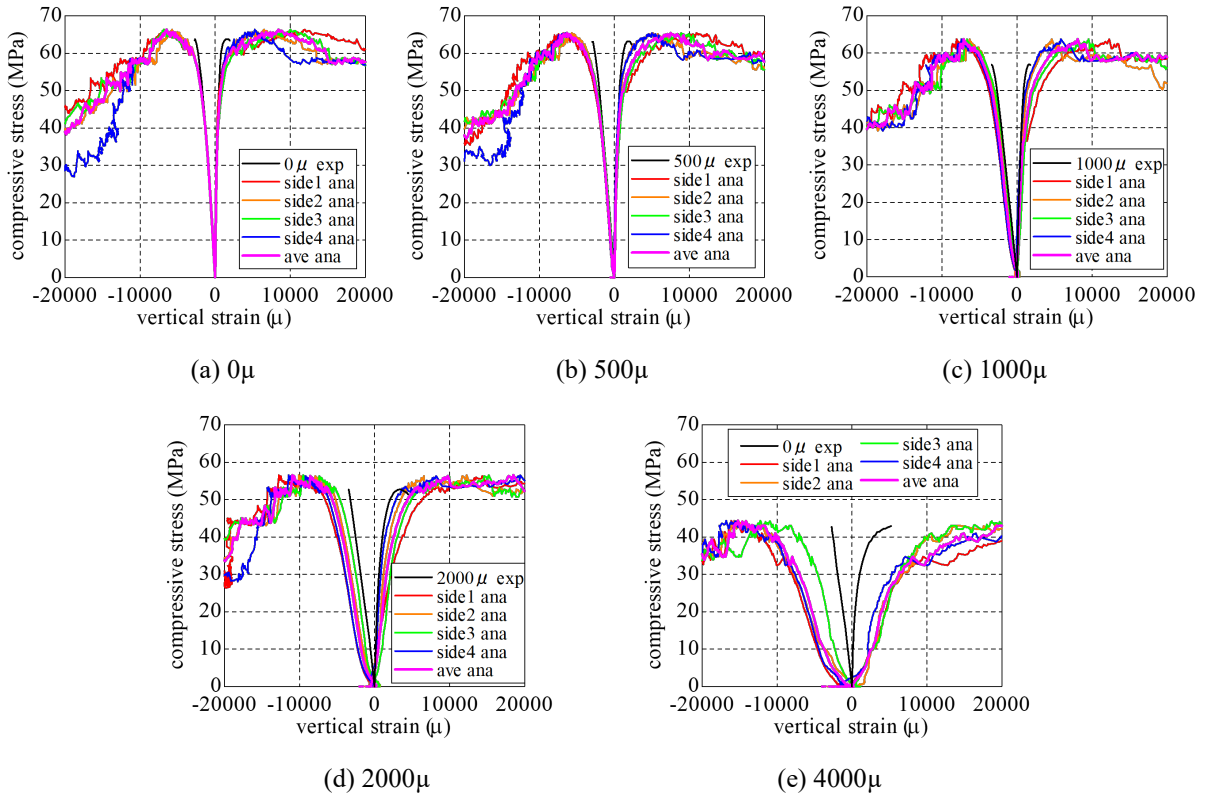


Figure 10: correspondence of compression stress and strain relationships [12]

compressive property can be evaluated simultaneously. Hereafter, the expansion crack distribution will be evaluate more precisely and the accuracy of proposed analysis will be improved to comprehend the mechanism of reduction of mechanical properties due to expansion crack by ASR.

## 12 CONCLUSIONS

In this study, the following knowledge can be obtained.

1. The analytical system coupled by reaction production model for ASR and mesoscopic structural analysis was developed. By

using proposed analysis, the change in expansion cracking behaviors and the change of compressive property can be evaluated simultaneously.

2. The tendency of expansion cracking behavior of each crack width can be reconstructed approximately while the time lag of starting point of expansion crack is not so close between experiment and analysis.
3. The proposed analysis can simulate the reduction of compression strength due to expansion crack by ASR.

## REFERENCES

- [1] Yamada K. et.al., 2013. ASR problems in Japan and a message for ASR problems in Thailand. , Journal of Thailand Concrete Association, Vol.1, No.2, pp.1-18.
- [2] Multon S., Sellier A., Martin C., 2009. Chemo–mechanical modelling for prediction of alkali silica reaction (ASR) expansion, Cement and Concrete Research, Vol.39, pp.490-500.
- [3] Ueda N., 2011. Study on damage prediction and structural performance evaluation of concrete structures deteriorated by alkali silica reaction, doctoral thesis, Nagoya University (in Japanese).
- [4] Takahashi Y. et.al., 2016. Scale-dependent ASR expansion of concrete and its prediction coupled with silica gel generation and migration, Journal of Advanced Concrete Technology, Vol.14, pp.444-463.
- [5] Alnaggar M., Cusatis G., Luzio G. D., 2013. Lattice Discrete Particle Modelling (LDPM) of Alkali Silica Reaction (ASR) deterioration of concrete structures, Cement and Concrete Composites, Vol.41, pp.45-59.
- [6] Diamond, S., 1989. ASR-Another Look at Mechanisms, Alkali -aggregate reaction 8th Inter. Conf. pp.83-94.
- [7] Uomoto T. and Furusawa Y., 1992. A Simple Model for Predicting Expansion in Mortar Bars due to Alkali-Silica Reaction, Concrete Research and Technology, Vol. 3, No. 1., pp.109-119 (in Japanese).
- [8] Sugimoto K.et.al., 2017. Fundamental study on ASR expansion behavior evaluation of RC member using RBSM, Proceedings of the Symposium on Developments in Prestressed Concrete, Vol. 26, pp.87-92 (in Japanese).
- [9] Kawai T., 1978. New discrete models and their application to seismic response analysis of structures, Nuclear Engineering and Design, 48, pp.207-229.
- [10] Bolander J.E., and Saito S., 1998. Fracture analyses using spring networks with random geometry, Engineering Fracture Mechanics, Vol. 61, 569-591.
- [11] Yamamoto Y. et.al., 2014. Crack propagation analysis of reinforced concrete wall under cyclic loading using RBSM, European Journal of Civil Engineering, Vol.18 (7), 780-792.
- [12] Sakai S. et.al., 2017. A study on strain distribution of cracked concrete due to ASR under compression loading, proceeding of JCI annual conference, Vol.39, No.1, pp.889-894 (in Japanese).